Rock Mech. Rock Engng. (2006) 39 (3), 233–253
DOI 10.1007/s00603-005-0070-7

Rock Mechanics and Rock Engineering
Printed in Austria

An Analytical Investigation of a Variable-Compliance-type Constitutive Equation

By

S. Okubo and **K. Fukui**

Department of Geo-system Engineering, University of Tokyo, Tokyo, Japan

Received June 1, 2004; accepted May 17, 2005
Published online September 23, 2005

Summary

A constitutive equation is proposed in which the compliance is assumed to monotonically increase as a load is applied. The primary feature of the constitutive equation is that the equation can be applied to various loading conditions such as constant stress rate, constant strain rate, creep, or relaxation. The second feature is that the equation has exact solutions under many loading conditions. The present paper shows the exact solutions for the constitutive equation and investigates the mutual relationships between the exact solutions for the different loading conditions. The third feature is that it is comparatively easy to find the constants in the constitutive equation. The present paper shows how to solve the constitutive equation for the constants, and the constants for some native Japanese rocks. The constitutive equation used in the present paper is extremely simple. Therefore, the equation can be easily implemented in almost any FEM code. It is likely that additional terms of the constitutive equation will prove necessary for practical usage. However, additional terms can be found very easily by finding higher-order approximations of experimental data.

Keywords: Rock, constitutive equation, analysis, visco-elasticity, creep, relaxation.

1. Introduction

Large underground structures and underground structures at great depth and with long service lives are currently under construction or being planned. Therefore, the time-dependent behavior of rock or rock mass has become increasingly important. The constitutive equation is a powerful tool with which to investigate the time-dependent behavior of rock for various purposes. For example, the long-term stability of underground structures can be simulated by computer programs using an appropriate constitutive equation. In addition, construction processes can be optimized with the aid of computer simulation. Prior to actual testing, new testing methods by which to investigate the visco-elastic properties of rock can be analyzed by computer to minimize

both cost and development time (Okubo et al., 1993). In addition, the constitutive equation is useful for examining and discussing the relationship between the results obtained under various loading conditions such as constant strain rate, constant stress (creep), and constant strain (relaxation). There are two requirements that must be satisfied in order for a constitutive equation to be applicable for these various purposes. First, a constitutive equation must be applicable under various loading conditions, such as constant strain rate, creep, and relaxation. Second, a constitutive equation must represent a wide range of mechanical responses, from the very ductile property of mudstone to the very brittle property of granite.

A number of constitutive equations have been derived for rocks (Desai, 1984). Among the various types of constitutive equations, a constitutive equation with the assumption of a steadily increasing compliance with time is discussed in the present paper (Okubo et al., 1987a, 1987b). The constitutive equation is not only comparatively simple in form and suitable to analytical investigation, but is also adaptable to a variety of loading conditions. However, almost none of the conventional constitutive equations allow analytical treatment of non-linear visco-elasticity. Although computer-supplied numerical solutions have enabled the investigation of a large number of conditions, the advantages of exact solutions are clear. Exact solutions are especially useful for the investigation and comparison of behaviors under differing loading conditions, for example, the results of creep experiments and compression tests.

In the following, the increasing rate of compliance λ is assumed to be expressible as the product of two arbitrary functions, $f(\lambda) \times g(\sigma)$, and the investigation is carried out without limitations on the form of $f(\lambda)$ or $g(\sigma)$. In addition, $f(\lambda)$ and $g(\sigma)$ are assumed to be represented by $a\lambda^m$ and σ^n, where rather than being constants for a particular rock type, m and n depend on, for example, the confining pressure (Okubo et al., 1987b). Once λ and σ are known, the location on the stress-strain curve can be identified and the rate of increase of λ at this location can be uniquely determined. A constant-$d\lambda/dt$ curve can then be drawn on the stress-strain graph, and this curve can be used as the basis for analytical investigation. Exact solutions can be also obtained for creep tests, relaxation tests, constant strain rate tests, or constant stress rate tests, and the exact relationships can be used to search for correlations.

The constitutive equation is intended to be used for estimating the long-term stability of underground structures such as nuclear waste repositories (JNC, 1999). Therefore, methods by which to find the constants in constitutive equations must be well established, and these methods should also be comparatively simple. Therefore, experimental identification of the constants will be described in the latter half of this paper. In addition, experimental identification of the constants for various types of rock will be demonstrated, and the variation of constants with confining pressure and water content will be described.

2. Constitutive Equations

The ratio of strain to stress, ε/σ, is defined as compliance λ. $d\lambda/dt$ is defined as being equal to the product of function $f(\lambda)$ with function $g(\sigma)$.

$$d\lambda/dt = f(\lambda)g(\sigma). \tag{1}$$

This encompasses the implicit assumption that $d\lambda/dt$ is determined only by the present values of λ and σ. Below, the terms in this constitutive equation will be described one by one.

Since stress is constant in a creep test, $g(\sigma)$ is constant. So if the $d\lambda/dt - \lambda$ curve is drawn, where $d\lambda/dt$ is represented by the vertical axis, and λ is represented by the horizontal axis, a curve is obtained for which the shape has no dependence on σ. In addition, $\lambda = \varepsilon/\sigma$ and ϵ are in direct proportion in the creep tests, so the same conclusion can be drawn for the $d\varepsilon/dt - \varepsilon$ curve. Previous research results have shown that $d\varepsilon/dt$ curves for which the shape is independent of stress can be obtained for Sanjome andesite, Kawazu tuff and other rocks (Yamaguchi et al., 1983; Okubo and Nishimatsu, 1986; Okubo et al., 1991). This is a strong confirmation of the reasoning behind Eq. (1). One of the features of this form of constitutive equation is that $f(\lambda)$, a function that is independent of stress, is easily obtained from the $d\varepsilon/dt - \varepsilon$ curve found in creep tests.

Next,

$$\tau = \int g(\sigma)dt \tag{2}$$

is defined, allowing Eq. (1) to be re-written as follows:

$$d\lambda/d\tau = f(\lambda). \tag{3}$$

Thus,

$$\int \frac{1}{f(\lambda)} d\lambda = \int d\tau. \tag{4}$$

As shown by Eqs. (3) and (4), λ can be described in terms of τ. Consequently, the $\lambda - \tau$ or $d\lambda/d\tau - \tau$ curve may be used as the master curves, regardless of the present value of σ.

For simplicity, let us continue the discussion with the test confined to the creep test. Here, σ is constant, so the following expressions apply:

$$t = \tau/g(\sigma), \tag{5}$$

$$d\lambda/dt = g(\sigma) \cdot d\lambda/d\tau. \tag{6}$$

Accordingly, the $\lambda - t$ curve at a creep stress of σ is obtained by shifting the master $\lambda - \tau$ curve by a factor of $1/g(\sigma)$ along the horizontal axis, and the $d\lambda/dt - t$ curve is obtained by shifting the $d\lambda/d\tau - \tau$ curve by $g(\sigma)$ and $1/g(\sigma)$ along the vertical and horizontal axes, respectively. If the $d\lambda/dt - t$ curve is plotted as a log–log graph, it can be plotted by shifting the master curve along a line having a slope of -1. Therefore, the lowest value on $d\lambda/dt$ would lie on a line with a slope of -1 on the log–log graph.

The quantities often observed in creep tests are the creep strain ϵ and its time rate of change, $d\varepsilon/dt$. Since λ and ϵ are directly proportional under constant stress, the $\varepsilon - t$ curve is obtained by shifting the master $\lambda - \tau$ curve by σ and $1/g(\sigma)$ along the vertical and horizontal axes, respectively. The following expression for creep strain rate is obtained:

$$d\varepsilon/dt = \sigma \cdot d\lambda/dt. \tag{7}$$

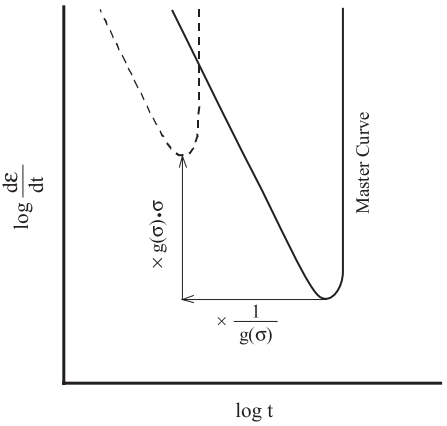

Fig. 1. Relationship between master curve (solid line) and creep strain rate curve obtained at creep stress σ (dashed line)

Thus, as shown in Fig. 1, the $d\varepsilon/dt$ curve can be obtained simply by shifting the master $d\lambda/d\tau - \tau$ curve by $g(\sigma) \times \sigma$ and $1/g(\sigma)$ along the vertical and horizontal axes. For the same reason, the points at which the creep strain rate are minimum for each creep stress and other corresponding points would lie along a straight line with the following slope:

$$-\frac{\log(g(\sigma)) + \log\sigma}{\log(g(\sigma))} \tag{8}$$

For example, for Sanjome andesite (Okubo et al., 1984), $g(\sigma) = K\sigma^{35}$ (K: a proportional constant). Equation (8) then is solved to obtain $-36/35 = -1.03$. It has been experimentally demonstrated that the points at which the creep strain rate are minimum lie approximately along a line with a slope of -1 on a log–log graph, as shown in Fig. 1 (Yamaguchi et al., 1983). The above discussion justifies the assumption of a constitutive equation having the form of Eq. (1).

3. Investigation of the Consequences of Constant $d\lambda/dt$

So far, we have assumed only the format of Eq. (1). Let us now assume, for the sake of the following discussion, that $f(\lambda)$ and $g(\sigma)$ take the following forms (Okubo et al., 1987a):

$$f(\lambda) = a\lambda^m, \tag{9}$$

$$g(\sigma) = \sigma^n. \tag{10}$$

These are then substituted into Eq. (1):

$$d\lambda/dt = a\lambda^m\sigma^n. \tag{11}$$

Let us also assume that the following ranges are permitted for parameters m and n:

$$-\infty < m < +\infty$$

$$1 \leq n < +\infty.$$

When n is 1, $d\lambda/dt$ is proportional to the stress. This indicates Newtonian viscosity. It is well known that there are visco-elastic materials for which n takes on values lower than 1, but n has been limited to values greater than or equal to 1 for the following discussion.

Equation (11) is simple in form. It has exact solutions under a variety of conditions, as will be shown below. Let us begin with a constant-$d\lambda/dt$ curve and examine its general behavior.

Substituting $d\lambda/dt = C$ into Eq. (11) and using the relationship $\varepsilon = \lambda\sigma$, we obtain:

$$\sigma = (C/a)^{1/(n-m)}\varepsilon^{-m/(n-m)} \tag{12}$$

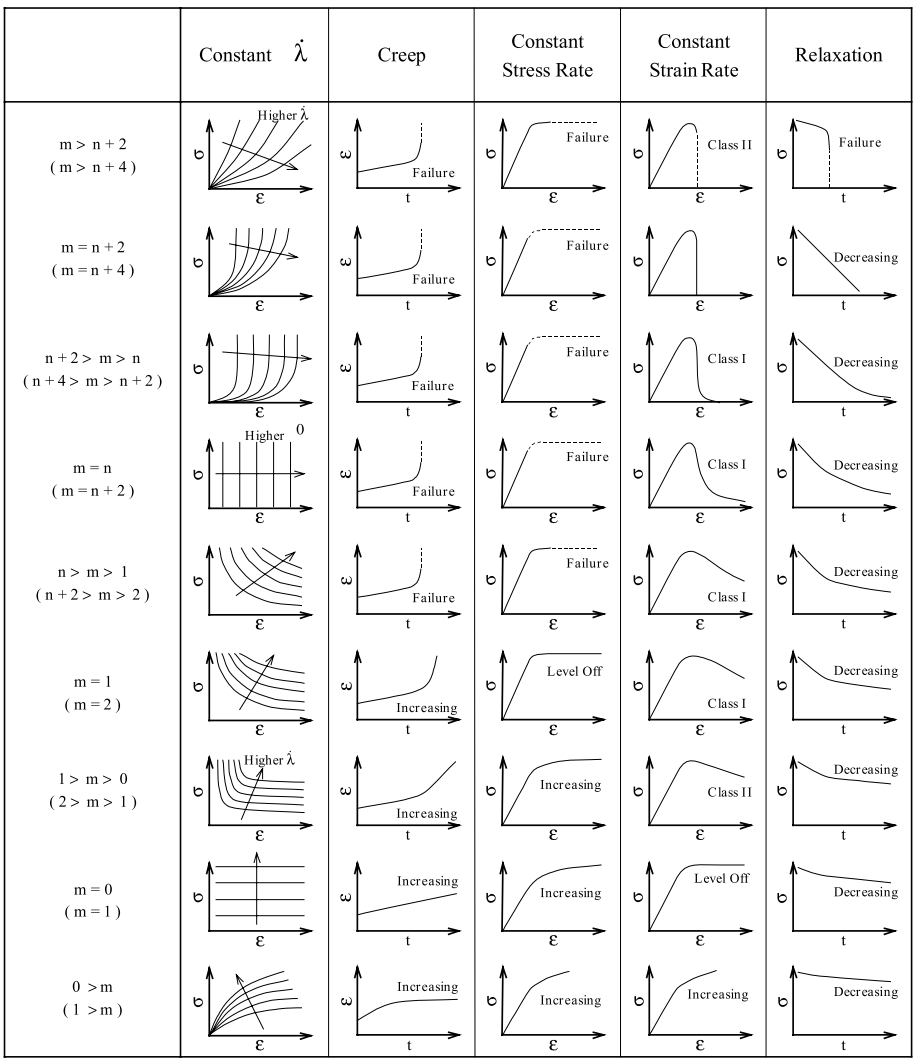

Fig. 2. Creep curve, stress-strain curve and relaxation curve according to magnitude m

The second column in Fig. 2 presents constant-dλ/dt curves on a stress-strain graph for nine magnitudes of m. As mentioned above, these may be interpreted as creep strain rate graphs, since ϵ and λ are proportional in creep tests in which constant stress is maintained.

Also, in relaxation tests,

$$d\varepsilon/dt = \sigma \cdot d\lambda/dt + d\sigma/dt \cdot \lambda = 0.$$

So, substituting dσ/dt $= -$C into Eq. (11), this relationship can be used to derive the following equation:

$$\sigma = (C/a)^{1/(n-m+2)} \varepsilon^{-(m-1)/(n-m+2)}. \tag{13}$$

Comparison with Eq. (12) indicates that the constant-dλ/dt curves in Fig. 2, replacing m and n with $(\mathrm{m}-1)$ and $(\mathrm{n}+1)$, respectively, can be used as the constant-stress reduction rate curves for relaxation tests. Since stress decreases with time in a relaxation test, the above C is the stress reduction speed and is itself positive. In conclusion, the constant-dλ/dt curve on the stress-strain graph expresses both the constant-creep strain rate curve and the constant-stress reduction rate curve in a relaxation test.

Let us next examine what happens when $\mathrm{m} > 0$. If a creep test is initiated at any arbitrary point on a stress-strain graph on the left side of Fig. 2 (constant-dλ/dt curves), the location on the graph moves to the right with the increasing strain, intersecting one after another curves with higher creep strain rate or higher dλ/dt. This means, of course, that the creep strain rate accelerates. When $\mathrm{m} = 0$, the constant creep-strain rate curve is a straight line parallel to the horizontal axis. In this case, the creep strain rate is constant. The constant-creep strain rate curve becomes concave downward when $\mathrm{m} < 0$. In this case, if a creep test is initiated at an arbitrary point on this graph, the location on the graph moves to the right, intersecting one after another curves of lower creep strain rate, i.e., the creep strain rate decreases with time.

Next, we will make some observations about the constant strain rate tests. Stress increases at a rate determined by the initial compliance, but asymptotically approaches the constant-creep strain rate curve corresponding to constant strain rate C as determined by the experimental conditions. The behavior up to this point does not vary significantly with the value of m, but thereafter is greatly influenced by m. If $\mathrm{m} > \mathrm{n}$, the constant-creep strain rate curve (constant-dλ/dt curve) is concave upward. For a given strain, the lower the stress, the higher the strain rate. Accordingly, once the material reaches the strength failure point (peak strength), failure accelerates and occurs catastrophically. The strength failure point coincides with the intersection between the constant-dλ/dt curve corresponding to strain rate C and the stress-strain curve. When m is lower than n and is positive, the creep strain rate curve is also concave upward. For a given strain, the lower the stress, the lower the strain rate. Thus, failure would be expected to proceed more slowly than in the case of $\mathrm{m} > \mathrm{n}$. When $\mathrm{m} = 0$, the constant-creep strain rate curve is described by a straight line parallel to the horizontal axis, so the stress does not increase beyond a certain point. Only the strain continues to increase. Thus, materials in which $\mathrm{m} > 0$ show distinct strength failure points or maximum levels of stress. When $\mathrm{m} < 0$, the creep strain rate curve is concave downward, and the stress continually increases approximately parallel to this curve.

Let us next consider relaxation tests. The constant-dλ/dt curve is now used, replacing m with $(m-1)$ and n with $(n+1)$, as the constant-stress reduction rate curve. The applicable ranges of m and n values for relaxation tests are noted in parentheses in the graph. When $m > n+2$, it is clear that the stress reduction rate accelerates as stress decreases due to relaxation. Ordinarily, relaxation tests show the stress diminishing at a decelerating rate with time, but it has been reported that in Class II rock, the stress reduction rate increases and eventually the rock fails (Okubo et al., 1987a). When $m = n+2$, the line becomes straight and parallel to the vertical axis, and relaxation proceeds at a constant stress reduction rate. When $m < n+2$, the stress reduction rate decreases with the reduction in stress, i.e., the stress reduction rate decreases continuously.

Let us also interpret a constant-dλ/dt curve as a constant-stress reduction rate curve for the constant stress rate test. The constant-stress reduction rate curve becomes parallel to the horizontal axis when $m = 1$. When $m > 1$, an abrupt increase in strain is predicted to occur once a certain stress is reached, and when $m < 1$, the constant-stress reduction rate curve slopes up to the right. Then, the stress increases along the corresponding constant-stress reduction rate curve with the same stress reduction rate as the stress rate in the constant stress rate test.

4. Exact Solution of Constitutive Equations

Table 1 lists the solutions to Eq. (11) obtained by creep tests, constant stress rate tests, constant strain rate tests and relaxation tests. The values in the table having the subscript 1 are the initial values in the tests. Figure 2 shows the trends for various cases of creep curves, stress-strain curves and relaxation curves.

The strain rates for the cases of creep are written as follows:

$$m > 1 \quad d\varepsilon^*/dt^* = \left\{ \frac{1}{1-(m-1)t^*} \right\}^{m/(m-1)}, \tag{14}$$

$$m = 1 \quad d\varepsilon^*/dt^* = \exp(t^*), \tag{15}$$

$$1 > m > 0 \quad d\varepsilon^*/dt^* = \{1+(1-m)t^*\}^{m/(1-m)}, \tag{16}$$

$$m = 0 \quad d\varepsilon^*/dt^* = 1, \tag{17}$$

$$m < 0 \quad d\varepsilon^*/dt^* = \left\{ \frac{1}{1+(1-m)t^*} \right\}^{1-\frac{1}{1-m}}, \tag{18}$$

where

$$t^* = a\lambda_1^{m-1}\sigma_1^n t,$$

$$\varepsilon^* = \varepsilon/\varepsilon_1 = \varepsilon/(\lambda_1\sigma_1).$$

As derived in the previous chapter, the strain rate accelerates when m is positive. It is also clear that for $m > 1$, failure occurs at $t^* = 1/(m-1)$, while for $m \leq 1$, failure

Table 1. Summary of exact solutions

Constitutive Equation	$\frac{d\lambda}{dt} = a\lambda^m\sigma^n$	$\lambda = \varepsilon/\sigma$	$a > 0$, $+\infty > m > -\infty$, $n \geq 1$	
Test (Condition) Initial Condition	Creep $(\sigma = \sigma_1)$ $\varepsilon = \varepsilon_1 = \lambda_1\sigma_1$	Constant Stress Rate $(\dot{\sigma} = C)$ $\lambda = \lambda_1$, $\sigma = 0$	Constant Strain Rate $(\dot{\varepsilon} = C)$ $\lambda = \lambda_1$, $\varepsilon = 0$	Relaxation $(\varepsilon = \varepsilon_1)$ $\sigma = \sigma_1 = \varepsilon_1/\lambda_1$
Symbol	$\varepsilon^* = \varepsilon/\varepsilon_1$ $t^* = a\ \lambda_1^{m-1}\sigma_1^n\ t$ $\beta = 1 - m$	$\varepsilon^* = \varepsilon/(\lambda_1\sigma)$ $t^* = \frac{a\ C^n t^{t+1}}{(n+1)\lambda_1^{1-m}}$ $\beta = 1 - m$	$\sigma^* = \sigma/(\varepsilon/\lambda_1)$ $t^* = -\frac{a\ C^n t^{n+1}}{(n+1)\lambda_1^{n-m+1}}$ $\beta = m - n - 1$	$\sigma^* = \sigma/\sigma_1$ $t^* = -a\ \lambda_1^{m-1}\sigma_1^n\ t$ $\beta = m - n - 1$
Solution	$\beta \neq 0$ $\varepsilon^* = (1 + \beta\ t^*)^{\frac{1}{\beta}}$ $\frac{d\varepsilon^*}{dt^*} = (1 + \beta t^*)^{\frac{1}{\beta}-1}$ $\beta = 0$ $\varepsilon^* = \exp(t^*)$ $\frac{d\varepsilon^*}{dt^*} = \exp(t^*)$		$\beta \neq 0$ $\sigma^* = (1 + \beta\ t^*)^{\frac{1}{\beta}}$ $\frac{d\sigma^*}{dt^*} = (1 + \beta\ t^*)^{\frac{1}{\beta}-1}$ $\beta = 0$ $\sigma^* = \exp(t^*)$ $\frac{d\sigma^*}{dt^*} = \exp(t^*)$	
Lifetime t_c	$m > 1$	$m > 1$	$m > 0$, $m \neq n + 1$*	$m > n + 1$
Strength σ_c	$t_c = \frac{1}{m-1} \times \frac{1}{a\lambda_1^{m-1}\sigma_1^n}$	$\sigma_c = \left(\frac{n+1}{m-1}\right)^{\frac{1}{n+1}} \lambda_1^{\frac{1-m}{n+1}} \times \left(\frac{C}{a}\right)^{\frac{1}{n+1}}$	$\sigma_c = \left(\frac{m}{n+1}\right)^{\frac{m}{(n+1)(n-m+1)}} \lambda_1^{-\frac{m}{n+1}} \times \left(\frac{C}{a}\right)^{\frac{1}{n+1}}$	$t_c = \frac{1}{m-n-1} \times \frac{1}{a\ \lambda_1^{m-1}\sigma_1^n}$

* At $m = n + 1$, $\sigma_c = \exp\left(-\frac{1}{n+1}\right) \cdot \lambda_1^{-1} \cdot \left(\frac{C}{a}\right)^{\frac{1}{n+1}}$

does not occur, even though the strain continues to increase. ''Failure'' here means that the strain becomes infinitely large in a finite time. If remaining lifetime T is defined as the time remaining until failure when $m > 1$, then Eq. (14) shows that the creep strain rate increases in proportion to $T^{-m/(m-1)}$. If $m \gg 1$, then the creep strain rate increases in proportion to T^{-1}, which fits the observations during creep tests (Okubo and Nishimatsu, 1986; Okubo et al., 1991; Fukui et al., 1989) and slope failure (Saito, 1980). Equation (18) shows that if m is negative, the strain rate decreases. If the absolute value of $m (m < 0)$ and t^* are very much greater than 1, then the creep strain rate is inversely proportional to the elapsed time. This result corresponds somewhat to the logarithmic law for creep (Cruden, 1971).

In constant stress rate tests, Eq. (14)–Eq.(18) also hold. Failure also occurs in this case at finite stress if $m > 1$. If $m \leq 1$, then the stress continues to increase, but failure does not occur.

The stress reduction rate in relaxation tests can be simplified when $m > n + 2$:

$$|d\sigma^*/dt^*| = \left\{ \frac{1}{1 - (m - n - 1)|t^*|} \right\}^{\frac{m-n-2}{m-n-1}}. \tag{19}$$

The stress reduction rate continues to increase with elapsed time, and failure occurs at $|t^*| = 1/(m - n - 1)$. In the same way, in constant strain rate tests, where Eq. (19) applies, if $m > n + 2$, then failure occurs at the same t^*. This clearly applies to Class II rock, in which it is not possible to maintain control in the post failure region. Also, from the results of Table 1, the stress reaches 0 at finite time in both relaxation and constant strain rate tests when $m > n + 1$. The stress does not reach 0 if $m \leq n + 1$.

5. Mutual Relationships between Test Results under Differing Loading Conditions

Below, the advantages of the exact solutions will be exploited in order to relate the results of tests under different loading conditions.

The strength under constant stress rate σ_{c1} and the strength under constant strain rate σ_{c2} can be found after performing a few calculations, as shown in Table 1. Note that both strengths are proportional to $C^{1/(n+1)}$. If the value of C for both quantities is chosen so that the strain rate is the same just after initiation of the test, the ratio between the two is given by

$$\frac{\sigma_{c1}}{\sigma_{c2}} \left\{ \frac{(n+1)^{n+1}}{(m-1)^{n-m+1} m^m} \right\}^{\frac{1}{(n-m+1)(n+1)}}, \quad m > 1,\ m \neq n + 1. \tag{20}$$

The value in brackets is less than 1 if $m > n + 1$ and is greater than 1 if $m < n + 1$, so σ_{c1} is always greater than σ_{c2}. This can also be shown to hold when $m = n + 1$. Many publications have described constant strain rate tests under servo-controlled testing machines (Swan et al., 1989). On the other hand, since there are not many reported examples of constant stress rate tests and the results from servo-controlled testing machines would be expected to vary greatly with response time of the machines (Okubo et al., 1993), it is necessary to wait for experimental results in order to verify Eq. (20). It will be difficult to verify Eq. (20) using Amsler or other types of

universal testing machines, because tests under these conditions fall somewhere between constant strain rate and constant stress rate tests.

The exact solutions for creep lifetime and relaxation lifetime are also shown in Table 1. Both bear an inverse relationship to $\sigma_1{}^n$. When the initial values of σ_1 and λ_1 are equal, the following relationship between the creep lifetime t_{c1} and relaxation lifetime t_{c2} can be derived:

$$\frac{t_{c1}}{t_{c2}} = \frac{m-n-1}{m-1}. \quad m > n+1. \tag{21}$$

Accordingly, the creep lifetime is always shorter than the relaxation lifetime. Although it is known that relaxation may lead to failure (Okubo et al., 1987a), currently available data are insufficient for quantitative investigation of Eq. (21).

Let us examine the relationship between the stress-dependence of creep lifetime and the strain rate-dependence of strength. If the strengths found at constant strain rates C_1 and C_2 are σ_{c1} and σ_{c2}, and the ratio between the strengths is γ, then the following equation is found from Table 1:

$$\gamma = \frac{\sigma_{c1}}{\sigma_{c2}} = \left(\frac{C_1}{C_2}\right)^{1/(n+1)}. \tag{22}$$

If the compliance is assumed to be identical at initiation of the creep test, and if the lifetimes at creep stresses of σ_{c3} and σ_{c4} are t_{c3} and t_{c4} and the ratio between the creep stresses is γ, then the following expression can be derived from Table 1:

$$\gamma = \frac{\sigma_{c3}}{\sigma_{c4}}\left(\frac{t_{c4}}{t_{c3}}\right)^{1/n}. \tag{23}$$

Since ordinarily $n \gg 1$, let us replace $n/(n+1)$ with 1, to obtain

$$\frac{C_1}{C_2} = \frac{t_{c4}}{t_{c3}}. \tag{24}$$

This indicates that if the strain rate is, for example, increased by a factor of 10, while the strength ratio is γ, the lifetime under a test with creep stress multiplied by the same ratio would be $1/10$ that of the life in the original test. Estimating creep lifetime is an essential problem in engineering. It will be extremely useful if the stress dependence of the creep lifetime can be predicted by the results of a constant strain rate test. Although there have not been many reports on this topic, the published experimental results (Okubo and Nishimatsu, 1986; Okubo et al., 1991) do not conflict with the argument presented above.

Let us move on to creep lifetime and the time to strength failure, τ_c, in a constant strain rate test. Let σ_c be the strength obtained in a test at constant strain rate C, and let t_c be the creep lifetime at a creep stress of $\gamma\sigma_c$. The following expression is obtained after some mathematical manipulation:

$$t_c = \frac{\gamma^{-n}\tau_c}{(m-1)\left(\frac{m}{n+1}\right)^{(m-1)/(n-m+1)}}. \tag{25}$$

This indicates that, in a creep test conducted at $\gamma \times 100\%$ of the strength, the creep lifetime is proportional to the time τ_c necessary to reach the strength failure point. The

strain at the strength failure point is proportional to $C^{1/(n+1)}$, so τ_c is proportional to $C^{-n/(n+1)}$. Therefore, when $n \gg 1$, both τ_c and the creep life are inversely proportional to the strain rate C used for measuring strength. Although creep tests are commonly reported as being ''carried out at 80% of the strength'', this is insufficient information, because it is also necessary to measure the strain rate when the strength is determined.

Let us next examine multi-stage creep. Let σ_k and Δt_k represent the k^{th} creep stress and the time over which this stress is applied. The solution can then be written as

$$\varepsilon = \left\{ \frac{1}{1-(m-1)a\lambda_1^{m-1}\sum(\sigma_k^n \Delta t_k)} \right\}^{1/(m-1)}. \tag{26}$$

Clearly, if we have

$$(m-1)a\lambda_1^{m-1}\sum(\sigma_k^n \Delta t_k) = 1,$$

then failure will occur. The above equation can be re-arranged to obtain

$$\sum \frac{\Delta t_k}{t_{ck}} = 1, \tag{27}$$

where

$$t_{ck} = \frac{1}{(m-1)a\lambda_1^{m-1}\sigma_k^n}.$$

As Table 1 shows, t_{ck} is the creep lifetime when the stress is σ_k. Equation (27) resembles Miner's rule (linear damage rule), which is often used to predict fatigue failure in metals. The authors found only a few experimental results (Yamaguchi et al., 2001) with which to confirm Eq. (27).

As shown in Fig. 3, Wawersik (1973) stated that if the stress-strain relationship obtained in a creep test is re-drawn on a stress-strain graph, either tertiary creep or an

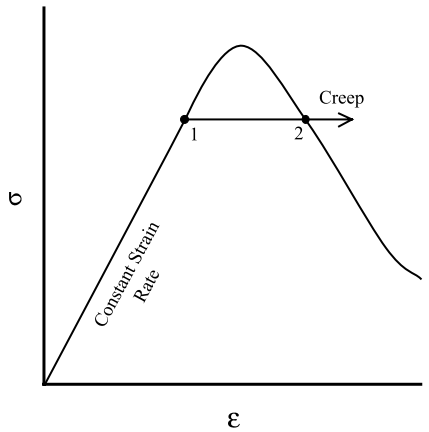

Fig. 3. Stress-strain curve and creep strain. Creep test begins from Point 1, creep strain extends to Point 2, where it intersects the stress-strain curve

abrupt acceleration in creep rate begins around the intersection between the stress-strain relationship in a creep test and the stress-strain curve found in compression tests. Another report (Fukui et al., 1989) stated that if the creep stress and creep strain one second before failure are plotted on a stress-strain graph, the plots will lie roughly along the stress-strain curve in the post failure region.

Let us further consider the latter finding. Let us assume that creep strain is steadily increased and compliance reaches λ_2 when the stress-strain relationship in the creep test intersects the stress-strain curve at a constant strain rate C. The lifetime remaining from this time until failure is then given by the following expression, according to Table 1:

$$t_c = \frac{1}{m-1}\frac{1}{a\lambda_2^{m-1}\sigma_2^n}, \tag{28}$$

where the subscript 2 indicates values at the intersection point, and σ_2 corresponds to the creep stress. After some manipulation, the relationship between σ and λ in the constant strain rate test can be simplified to the following when $m \neq n+1$:

$$\sigma = \left(\frac{C}{a}\frac{n+1}{n-m+1}\frac{\lambda^{n-m+1}-\lambda_1^{n-m+1}}{\lambda^{n+1}}\right)^{1/(n+1)}. \tag{29}$$

Since this expression also holds at the intersection point, we may replace σ with σ_2 and λ with λ_2 in Eq. (28) to obtain

$$t_c = \frac{n-m+1}{(m-1)(n+1)}\frac{\lambda_2\sigma_2}{C}\frac{1}{1-(\lambda_1/\lambda_2)^{n-m+1}}, \tag{30}$$

$\lambda_2\sigma_2$ is the strain ε_2 at the intersection point. If t_2 is the time to the intersection point in a constant strain rate test, $\lambda_2\sigma_2 = Ct_2$. Then, we obtain

$$t_c = \frac{n-m+1}{(m-1)(n+1)}\frac{t_2}{1-(\lambda_1/\lambda_2)^{n-m+1}}. \tag{31}$$

The following expression to calculate the creep strain rate at the intersection point can be found with some manipulation:

$$d\varepsilon/dt = C\frac{n+1}{n-m+1}\left\{1-\left(\frac{\lambda_1}{\lambda_2}\right)^{n-m+1}\right\}. \tag{32}$$

Considering both Eq. (30) and Eq. (32), t_c and $d\varepsilon/dt$ depend on the strain rate C used in obtaining the basic stress-strain curve. In other words, t_c is inversely proportional and $d\varepsilon/dt$ is directly proportional to C. As is the case when a creep stress of 80% of strength has been applied to Sanjome andesite and $n-m+1$ is large, $(\lambda_1/\lambda_2)^{n-m+1}$ can be ignored. Equations (31) and (32) are then given as follows:

$$t_c = \frac{n-m+1}{(m-1)(n+1)}t_2, \tag{33}$$

$$d\varepsilon/dt = C\frac{n+1}{n-m+1}. \tag{34}$$

For the case of Sanjome andesite, if $n = 35$, $m = 20$ and $t_2 = 100$ s, Eq. (33) is calculated to be approximately 2 s, which is not significantly different from the result reported by Fukui et al. (1989). Inserting the same m and n values into Eq. (34), we obtain a $d\varepsilon/dt$ of approximately 2C. This will be confirmed or disproved by future testing.

6. Constants in the Constitutive Equations

6.1 How to Identify Constants

In order to solve Eq. (11) under a uniaxial compression test, values are required for λ_1, the initial λ, and the three constants n, m and a in the constitutive equation.

Let us begin with the identification of λ_1. As shown in Table 2, λ_1 is the reciprocal of the tangential Young's modulus obtained at 50% of the peak strength found in the compression test. For some rock types, the stress-strain curve becomes non-linear at rather low stress levels. An additional term may have to be inserted into the right-hand side of Eq. (11) in order to accommodate the deformation properties of such rocks. This however is beyond the scope of the present report.

The value of n may be determined from creep, constant stress rate, constant strain rate or relaxation tests. Once the relationship between creep stress σ_1 and lifetime t_c as been determined from creep tests, n can be calculated using the following equation from Table 2:

$$n = \frac{\delta(\ln t_c)}{\delta(\ln \sigma_1)}. \tag{35}$$

The slope of a straight line drawn through lifetime-creep stress values on a log–log chart will provide this value. This will apply for values of m greater than 1. For $m \leqslant 1$, only strain hardening will occur, not failure, so t_c will not exist. For these

Table 2. How to find constants in a constitutive equation

Constitutive Equation	$\frac{d\lambda}{dt} = a\,\lambda^m\sigma^n$	$\lambda = \frac{\varepsilon}{\sigma}$	$a > 0$, $+\infty > m > -\infty$, $n \geq 1$	
Test (Condition)	Creep ($\sigma = \sigma_1$)	Constant Stress Rate ($\dot{\sigma} = c$)	Constant Stress Rate ($\dot{\varepsilon} = c$)	Relaxation ($\varepsilon = \varepsilon_1$)
Initial Condition	$\varepsilon = \varepsilon_1 = \lambda_1\sigma_1$	$\lambda = \lambda_1$, $\sigma = 0$	$\lambda = \lambda_1$, $\varepsilon = 0$	$\sigma = \sigma_1 = \varepsilon_1/\lambda_1$
λ_1	inverse of 50% tangential Young's modulus			
n	$m > 0$	$m > 1$	$m > 0$, $m \neq n + 1$	$m > n + 1$
	$\frac{\delta(\ln t_c)}{\delta(\ln \sigma_1)}$	$\frac{\delta(\ln c)}{\delta(\ln \sigma_c)} - 1$	$\frac{\delta(\ln c)}{\delta(\ln \sigma_c)} - 1$	$\frac{\delta(\ln t_c)}{\delta(\ln \sigma_1)}$
m	Not feasible		Refer to Fig. 4	Not feasible
a	$m > 1$	$m > 1$	$m > 0$, $m \neq n + 1$	$m > n + 1$
	$\frac{1}{m-1}\lambda_1^{1-m}$ $\cdot \sigma_1^{-n} \cdot t_c^{-1}$	$\left(\frac{n+1}{m-1}\right)\lambda_1^{1-m}$ $\cdot \sigma_c^{-(n+1)} \cdot c$	$\left(\frac{m}{n+1}\right)^{\frac{m}{n-m+1}}\lambda_1^{-m}$ $\cdot \sigma_c^{-(n+1)} \cdot c$	$\frac{1}{m-n-1}\lambda_1^{1-m}$ $\cdot \sigma_1^{-n} \cdot t_c^{-1}$

σ_c: peak strength, t_c: lifetime, $\delta(\ln t_c)$: finite difference of $(\ln t_c)$

rock types, one must resort to numerical trial-and-error methods to obtain calculated results matching the experimentally determined creep curves. Numerical trial-and-error must also be used with other experiments described below if failure does not occur.

If a relationship between loading rate C and peak strength σ_c is found in constant stress rate tests, n can be calculated using the equation shown in Table 2. This is valid for $m > 1$. For $m \leqslant 1$, failure does not occur, so peak stress σ_c does not exist. n can be calculated using the equation in Table 2 for constant strain rate tests; this is valid for $m > 0$. For $m \leqslant 0$, failure does not occur. In relaxation tests, n can be calculated using the expression in Table 2 when $m > n + 1$. If m is less than $(n + 1)$, then no failure of the test sample occurs. The time from test initiation to failure t_c depends on σ_1, the stress at initiation of relaxation, so this relationship can be used to find n.

Here, m can be found using a constant strain rate test. Theoretically, m is also calculable from other tests, but this is actually quite difficult. In addition, m is related to the slope of the stress-strain curve after the peak strength observed in the constant strain rate test. Numerical iteration until the experimental results match the calculated results could be used to determine m, but this is somewhat troublesome. Figure 4 suggests a simple way to find m. Here, point A is the intersection between the tangent to the stress-strain line at point B, which indicate 50% of peak strength, and a horizontal line at $\sigma =$ peak strength. Point C is determined by setting the lengths of AB and AC to be equal. The angle α' measured clockwise from the horizontal line $(\sigma = \sigma_c)$ is drawn as shown in the graph, and $\alpha = \arctan(\tan\alpha'/\tan\theta)$ is calculated. Of course, if the slope θ of the tangent at the 50% strength point is 45°, then α' is the same as α. The relationship between the α found here and m/n is shown in Fig. 5. Also, if α is negative, the material shows no peak strength. The stress-strain curve continues to increase to the right.

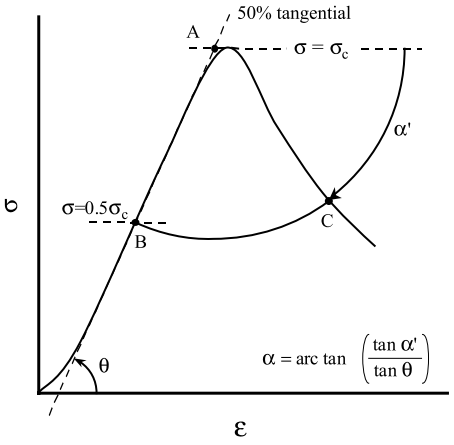

Fig. 4. How to find α, indicator of the slope of the stress-strain curve in the post failure region. Procedure #1 Find Point A, which is located at the intersection of the tangent at 50% strength and $\sigma = \sigma_c$. Procedure #2 Find intersection C by drawing an arc of radius AB centered at A. Procedure #3 Define angle α' between straight line AC and $\sigma = \sigma_c$. Procedure #4 Calculate $\alpha = \arctan(\tan\alpha'/\tan\theta)$

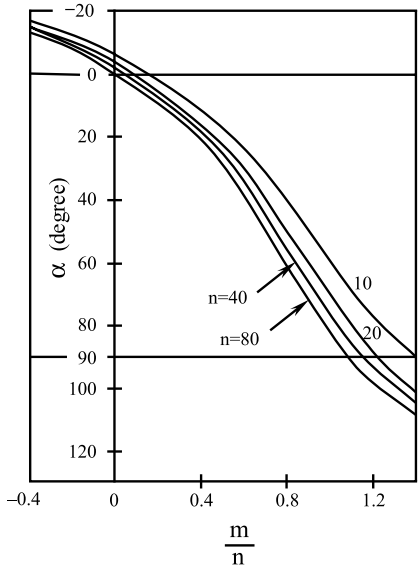

Fig. 5. Relationship between α and m/n

By substituting the values for λ_1, n and m and the results of the tests (for example, the loading rate C and peak strength σ_c from the constant strain rate test) into the expression in Table 2, a can be found.

The above explanation is a simple explanation of the use of the constitutive equations for the uniaxial compression test, but the methods for finding λ_1, a, m, and n do not differ greatly under the condition of confining pressure. The differential strain and differential stress must simply be substituted for the strain ϵ and stress σ.

6.2 Influence of Confining Pressure

Table 3 lists the values for rock reported in previous studies (Okubo et al., 1991, 1990; He et al., 1990). The peak strength shown for differential stress (maximum differential stress) and λ_1 were identified in the constant strain rate test. The value of n in the table was calculated using the expression in Table 2 by using multiple strain rates for several constant strain rate tests. In addition, n was calculated for some rock types using the results of creep tests. Compared to the values found in the constant strain rate tests no large differences were found. Also, α was found by the method shown in Fig. 4. The variables a and m in the constitutive equation were easily found using the expression in Table 2 and Fig. 5.

Figure 6 shows the degree of change caused by the confining pressure, with n on the vertical axis and α on the horizontal axis. Larger n indicates a weaker time-dependence. For example, the loading rate-dependence of peak strength in the constant strain rate test falls with increasing n, and the material behavior approaches plastic. In contrast, the lower the α value, the more gentle the falling slope of the stress beyond peak strength, i.e. the greater the ductility. Although we considered

Table 3. Identified rock constants

Sample rock	Experimental condition	Peak strength (MPa)	$\lambda 1$ (1/GPa)	n	α (°)
Inada granite	Uniaxial compression (Air Dried)	193	1/37.6	51	99
	Uniaxial compression (Water saturated)	185	1/37.6	38	99
	Triaxial compression (Air Dried)				
	Confining pressure 5 MPa	274	1/39.7	72	62
	10 MPa	348	1/39.7	92	56
	20 MPa	422	1/40.4	112	42
	40 MPa	556	1/40.4	147	38
Sanjome andesite	Uniaxial compression (Air Dried)	93.9	1/9.3	37	91
	Uniaxial compression (Water saturated)	73.4	1/8.4	28	88
	Triaxial compression (Air Dried)				
	Confining pressure 5 MPa	141	1/13.7	48	66
	10 MPa	167	1/14.2	56	48
	20 MPa	207	1/14.2	70	27
	40 MPa	244	1/14.5	83	17
Kawazu tuff	Uniaxial compression (Air Dried)	33.3	1/6.3	57	68
	Uniaxial compression (Water saturated)	22.3	1/5.2	37	74
	Triaxial compression (Air Dried)				
	Confining pressure 2.5 MPa	36.0	1/6.4	62	9
	5 MPa	37.7	1/6.4	64	3
	10 MPa	39.5	1/6.4	67	0
Oya tuff	Uniaxial compression (Air Dried)	12.2	1/2.7	35	32
	Uniaxial compression (Water saturated)	5.63	1/1.3	16	31
Tage tuff	Uniaxial compression (Air Dried)	16.8	1/3.6	42	20
	Uniaxial compression (Water saturated)	9.74	1/2.5	23	34
	Uniaxial tension (Air Dried)	1.87	1/2.8	42	19
Aki yoshi marble	Uniaxial compression (Air Dried)	124	1/35.1	63	38
Izumi sandstone	Uniaxial compression (Air Dried)	214	1/25.0	61	102

using m or m/n for the horizontal axis, α was chosen as this appears to be more direct and easier to grasp.

Let us first consider Inada granite (○), which showed increasingly ductile behavior and sharply decreasing time-dependence with increased confining pressure of 5, 10, 20 and 40 MPa in comparison with test results at atmospheric pressure. It is well known that ductility is increased by increasing confining pressure, but few reports (Green et al., 1972; Kranz, 1980; Blanton, 1981) have taken up time-dependence. The • symbols represent the results for Sanjome andesite, which showed only a slight

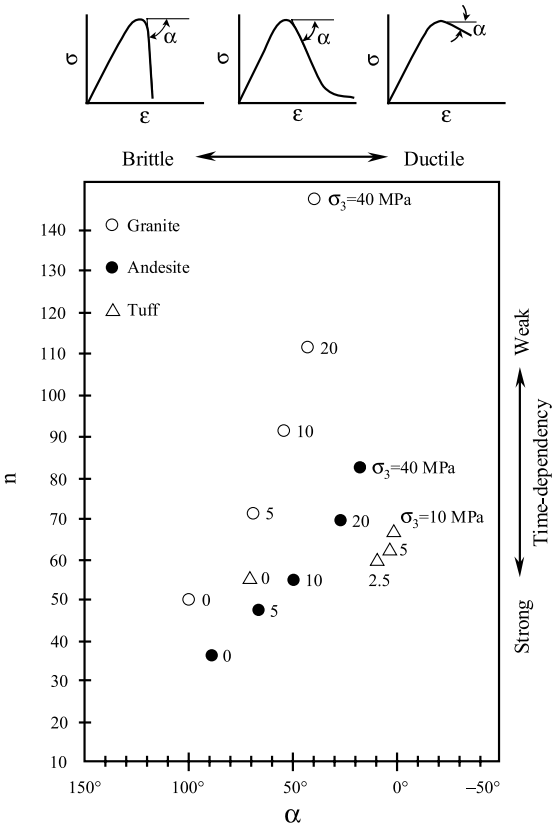

Fig. 6. Relationship between n, indicator of time-dependence, and α, indicator of ductility/brittleness (affected by confining pressure σ_3); ○: Inada granite ●: Sanjome andesite Δ: Kawazu tuff

change in n due to confining pressure, but a much more noticeable change in α than in granite. The Δ symbols represent Kawazu tuff, which also showed a slight change in n, but a noticeable change in α.

6.3 Influence of Water Content

Steel and other industrial materials are known to be sensitive to their environments, and the speed of corrosion is largely determined by the presence or absence of water. In many cases, however, water infiltration is extremely low, and it suffices to discuss changes near the surface. On the other hand, many rocks allow water to penetrate into the interior, and the presence of water has a dramatic effect on their mechanical properties (Sano, 1981; Lajtai et al., 1987).

Figure 7 shows the results of several constant strain rate tests under uniaxial compression. ○ indicates the results under an air-dried condition, and ● indicates the results under the water-saturated condition. The results clearly show that, despite

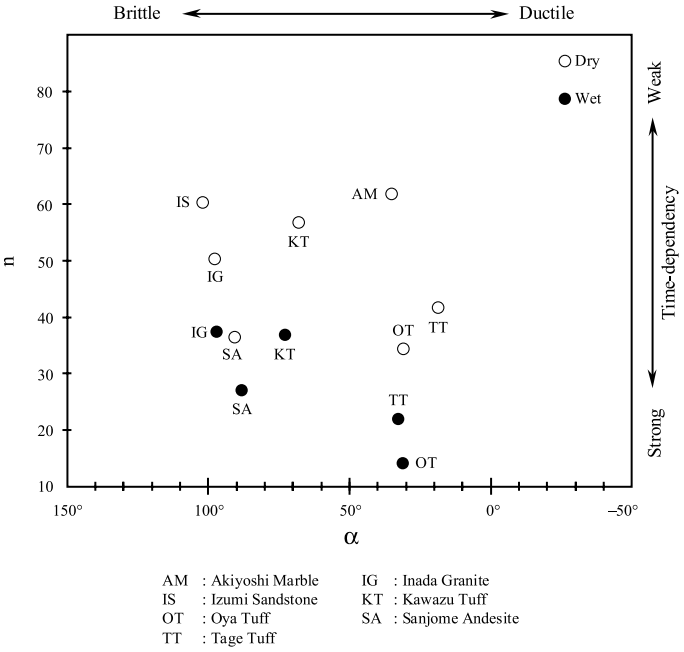

Fig. 7. Relationship between n, indicator of time-dependence, and α, indicator of ductility/brittleness (affected by water content); ○: Air-dried condition ●: Water-saturated condition

the occurrence of some scatter, there is a strong tendency for the figures from the air-dried samples to be higher than those from the water-saturated samples.

Figure 8 provides a hypothesis for future research objectives. Here, B, C_H and C_L are rock mass ratings (JSEGPC, 1992) created according to the method of the Central Research Institute of the Electric Power Industry (CRIEPI). Two further hypotheses were added in order to complete this figure: #3, if the temperature is high, the time-

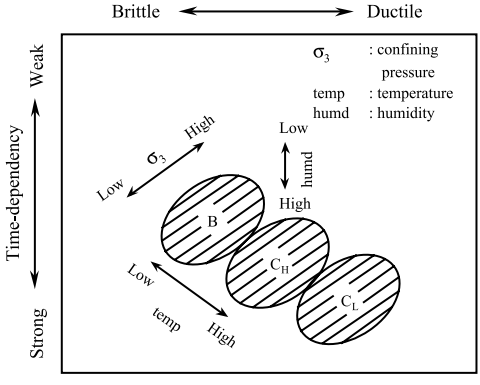

Fig. 8. Relationships between n and α for hypothetical rock types under the following four hypotheses: #1 the graph is shifted up and right by an increase in confining pressure; #2 the graph is shifted down by an increase in water content; #3 the graph is shifted right and down by an increase in temperature; and #4 the graph is shifted right and down by a reduction in strength. B, C_H and C_L are rock mass ratings according to the method of CREIPI. B, for relatively better rock mass, is followed by C_H and C_L

dependence increases and the material shows ductile properties (Heuze, 1983); and #4, the weaker the rock, the higher the time-dependence and the greater the ductility. These are the primary hypotheses currently planned for investigation in the laboratory, in situ, or by numerical simulations. It will be instructive to determine which hypothesis most closely fits the actual behavior of the materials.

7. Conclusions

Constitutive equations assuming a steady increase in compliance were investigated. Changes in compliance were examined by releasing load during constant strain rate tests and examining the characteristics during load release. Both increased compliance and irrecoverable strain were observed in actual rocks (He et al., 1990). The constitutive equation must therefore separate the increase of compliance from the increase of irrecoverable strain in order to handle the alternative strain fluctuation. However, it is rare for strain in underground structures of rock to decrease and, therefore, it is sufficient to investigate the constitutive equation presented herein.

The simplest way to justify Eq. (1) is to show that the shape of the $d\varepsilon/dt - \varepsilon$ curve is independent of creep stress in creep tests. This has been shown under relatively high stresses in Sanjome andesite and Kawazu tuff, but it is necessary to conduct further investigations using other types of rock under lower stresses and various confining pressures.

An exact solution of Eq. (11) for creep tests, relaxation tests, constant strain rate tests, or constant stress rate tests is shown, assuming the formats for $f(\lambda)$ and $g(\sigma)$ provided in Eqs.(9) and (10). The advantages of the exact solution were exploited in order to investigate the mutual relationships between the various kinds of tests. The following is a summary of the key findings of the present study:

1) A close relationship was derived in Eq. (24) between the dependence of strength in constant strain rate tests on loading rate and the dependence of lifetime in creep tests on creep stress. Once one relationship is known, the other can be derived.
2) A close relationship was derived in Eq. (25) between the creep lifetime and the time to strength failure in the constant strain rate test.
3) An equation (Eq. (27)) resembling Miner's rule was derived for cumulative damage during multi-stage creep.
4) Remaining lifetime and strain rate were derived for the case in which the creep strain is equal to the width of the stress-strain curve at the corresponding stress level. These are given as Eqs. (31) and (32).

Both visco-elasticity and time-dependency have long attracted the interest of materials researchers, but until now these have remained unclear with respect to rocks. Previous research has been phenomenologically oriented and fragmentary, focusing on experimental findings. There are severe gaps, such as the mutual relationships between experimental results under different conditions, discussed above in Chapter 5. The reason for this is the lack of a clear paradigm encompassing the known phenomena, which is necessary for an integrated approach to investigation.

Table 2 lists the methods for finding the constants in the constitutive equation. In many cases, the constant strain rate test is the simplest means. The stress and the strain are to be collected during this test. The order of finding constants is: λ_1, n, m, and a.

Being the reciprocal of the tangent Young's modulus at the 50% line, λ_1 is found first. Next, n is found using the change in peak strength when changing the loading rate. At the same time, as shown in Fig. 4, the value for α is found, which provides m/n. Finally, λ_1, n, m, the loading rate C, and the peak strength σ_c are used to calculate a.

Constants were experimentally determined for a number of rock types, and these are listed in Table 3. The influences of confining pressure and water content have been presented in Figs. 6 through 8, in which the vertical axes represent n (an indicator of time-dependence) and horizontal axes represent α (an indicator of ductility/brittleness). The following trends are visible in the figures: (1) the graph is shifted to the right by increases in confining pressure, and (2) the graph is shifted downward by the presence of water.

The constitutive equation used in the present paper is extremely simple, and can therefore be easily implemented in almost any FEM code for static linear elasticity (Okubo et al., 1987b). In addition, numerical calculation to estimate the long-term stability of underground structures can be readily performed with the code. For example, numerical simulation results for long-term tunnel deformation were presented in the second report of JNC (1999). Although it is likely that additional terms of the constitutive equation will prove necessary for practical usage, these can be added very easily by simply finding a higher-order approximation of the experimental data (Okubo et al., 2003). Thus, in the uniaxial stress state, the constitutive equation with additional terms can reproduce a great variety of complete stress-strain curves and creep curves that were obtained experimentally, and the results calculated by various types of constitutive equations or formally proposed models can be reproduced.

Acknowledgement

The authors extend their deepest gratitude to Prof. Em. Yuichi Nishimatsu of the University of Tokyo for his invaluable advice during this project.

References

Blanton, T. L. (1981): Effect of strain rates from 10^{-2} to 10 sec^{-1} in triaxial compression tests on three rocks. Int. J. Rock Mech. Min. Sci. Geomech. Abstr. 18, 47–62.

Cruden, D. M. (1971): The form of the creep law for rock under uniaxial compression. Int. J. Rock Mech. Min. Sci. 8, 105–126.

Desai, C.S., Siriwardane, H. J. (1984): Constitutive laws for engineering materials with emphasis on geologic materials. Prentice-Hall Int., London.

Fukui, K., Okubo, S., Nishimatsu, Y. (1989): Creep behavior of rock under uniaxial compression. J. Min. Metall. Inst. Japan 105(7), 521–526 (in Japanese).

Green, S. J., Leasia, J. D., Perkins, R. D., Jones, A. H. (1972): Triaxial stress behavior of Solenhofen limestone and Westerly granite at high strain rates. JGR 77(20), 3711–3724.

He, C., Okubo, S., Nishimatsu, Y. (1990): A study on the class II behaviour of rock. Rock Mech. Rock Engng 23, 261–273.

Heuze, F. E. (1983): High-temperature mechanical, physical and thermal properties of granitic rocks-a review. Int. J. Rock Mech. Min. Sci. Geomech. Abstr. 20(1), 3–10.

JNC (Japan Nuclear Cycle Development Institute) (1999): Second progress report on research and development for the geological disposal of HLW in Japan. JNC TN1400 99-022(IV), 355–362 (in Japanese).

JSEGPC (The Japan Society of Engineering Geology Publication Committee) (1992): Rock mass classification in Japan. Engng. Geol. Special Issue, 18–19.

Kranz, R. L.: The effects of confining pressure and stress difference on static fatigue of granite. JGR 85(B4), 1854–1866.

Lajtai, E. Z., Schmidtke, R. H., Bielus, L. P. (1987): The effect of water on the time-dependent deformation and fracture of a granite. Int. J. Rock Mech. Min. Sci. Geomech. Abstr. 24(4), 247–255.

Okubo, S., Shin, K., Nishimatsu, Y. (1984): Mathematical model of crack growth for Sanjome andesite. J. Soc. Materials Sci. 33(370), 882–887 (in Japanese).

Okubo, S., Nishimatsu, Y. (1986): Creep behaviour and constitutive equation of Sanjome andesite and Kawazu tuff. J. Min. Metall. Inst. Japan 102(7), 395–400 (in Japanese).

Okubo, S., He, C., Nishimatsu, Y. (1987a): Time dependent behaviour in uniaxial compression – Rheological behaviour of rock in post-failure region (1st Report). J. Min. Metall. Inst. Japan 103(3), 177–181 (in Japanese).

Okubo, S., Nishimatsu, Y., Ogata, Y. (1987b): Simulation of rock deformation around roadway by non-linear rheological model. J. Min. Metall. Inst. Japan 103(5), 293–296 (in Japanese).

Okubo, S., Nishimatsu, Y., He, C. (1990): Loading rate dependence of class II rock behaviour in uniaxial and triaxial compression. Tests – An application of a proposed new control method. Int. J. Rock Mech. Min. Sci. Geomech. Abstr. 27(6), 559–562.

Okubo, S., Nishimatsu, Y., Fukui, K. (1991): Complete creep curves under uniaxial compression. Int. J. Rock Mech. Min. Sci. Geomech. Abstr. 28(1), 77–82.

Okubo, S., Fukui, K., Nishimatsu, Y. (1993): Control performance of servo-controlled testing machines in compression and creep test. Int. J. Rock Mech. Min. Sci. Geomech. Abstr. 30(3), 247–255.

Okubo, S., Fukui, K., Hashiba, K. (2003): Extension of constitutive equation of variable compliance type and its validation based on uniaxial compression and tension tests of Sanjome andesite. J. Min. Metall. Inst. Japan 119(9), 541–546 (in Japanese).

Saito, M. (1980): SEMI logarithmic representation for forecasting slope failure. Proc Int. Symp. Landslides. New Delhi, Vol. 1, 321–324.

Sano, O. (1981): Influence of strain rate on dilatancy and strength of Oshima granite under uniaxial compression. JGR 86(B10), 9299–9311.

Swan, G., Cook, J., Bruce, S., Meehan, R. (1989): Strain rate effects in Kimmerridge bay shale. Int. J. Rock Mech. Min. Sci. Geomech. Abstr. 26(2), 135–149.

Yamaguchi, T., Okubo, S., Nishimatsu, Y., Koizumi, S. (1983): The creep behavior of Sanjome andesite under confining pressure – The time-dependent mechanical behavior of rock (2nd Report). J. Min. Metall. Inst. Japan 99(12), 1029–1034 (in Japanese).

Yamaguchi, T., Okubo, S., Maranini, E. (2001): Distribution of strength and creep failure time of Inada granite under confining pressure. Proc. 2001 ISRM Int. Symp.-2nd Asian Rock Mech. Symp. Beijing, 177–180.

Wawersik ,W. R. (1973): Time-dependent rock behavior in uniaxial compression. Proc 14th US Symp. Rock Mech. University Park, PA. ASCE, New York 85–106.

Authors' address: Dr. S. Okubo, Department of Geo-systems Engineering, University of Tokyo, 7-3-1 Hongo, Bunkyo 113-8656, Tokyo, Japan; e-mail: ttokubo@geosys.t.u-tokyo.ac.jp